Full paper

Applied Organometallic Chemistry

Received: 8 April 2016 Revised: 6 May 2016 Accepted: 8 June 2016 Published online in Wiley Online Library

(wileyonlinelibrary.com) DOI 10.1002/aoc.3551

Catalytic promiscuity of an iron(II)–phenanthroline complex

Abhranil De[a], Mamoni Garai[a], Hare Ram Yadav[b], Angshuman Roy Choudhury[b] and Bhaskar Biswas[a]*

A mononuclear iron(II) complex, $[Fe(phen)_3]Cl_2$ (1) (phen =1,10-phenanthroline), has been synthesized in crystalline phase and characterized using various spectroscopic techniques including single crystal X-ray diffraction. Crystal structure analysis revealed that 1 crystallizes in a monoclinic system with C2/m space group. Complex 1 acts as a functional model for a biomimetic catalyst promoting the aerobic oxidation of 3,5-di-*tert*-butylcatechol (3,5-DTBC) through radical pathways with a significant turnover number (k_{cat} =3.55 × 10^3 h^{-1}) and exhibits catechol dioxygenase activity towards the same 3,5-DTBC substrate at room temperature in oxygen-saturated ethanol medium. The existence of an isobestic point at 610 nm from spectrophotometric data indicates the presence of Fe^{3+} −3,5-DTBC adduct favouring an enzyme–substrate binding phenomenon. Upon stoichiometric addition of 3,5-DTBC pretreated with two equivalents of triethylamine to the iron complex, two catecholate-to-iron(III) ligand-to-metal charge transfer bands (575 and 721 nm) are observed and the in situ generated catecholate intermediate reacts with dioxygen (k_{obs} =9.89 × 10^{-4} min^{-1}) in ethanol medium to afford exclusively intradiol cleavage products along with a small amount of benzoquinone, and a small amount of extradiol cleavage products, which provide substantial evidence for a substrate activation mechanism. Copyright © 2016 John Wiley & Sons, Ltd.

Additional supporting information may be found in the online version of this article at the publisher's web site.

Keywords: catecholase activity; catechol dioxygenase activity; iron(II); phenanthroline; X-ray structure

Introduction

The synthesis and reactivity studies of transition metal complexes as structural and functional models for metalloenzymes with oxidase and oxygenase activity are of particular interest for the development of bio-inspired catalysts.[1–3] A number of important oxidative transformations are carried out by iron enzymes utilizing dioxygen as an oxygen source. Iron is therefore ideally suited for its many roles in biology including the transport and storage of dioxygen (O_2) and the catalysis of numerous reactions that utilize dioxygen.[4–7] Catechol dioxygenases are a class of non-heme iron enzymes that catalyse the oxidative cleavage of catechols. They are divided into two subclasses: the intradiol dioxygenases, which utilize a non-heme iron(III) cofactor in catalysing the cleavage of the carbon–carbon bond between the two catechol oxygens; and the extradiol dioxygenases, which utilize a non-heme iron(II) cofactor in catalysing the cleavage of the carbon–carbon bond adjacent to the catechol oxygens.[8–17] Even though intradiol cleavage is the less common route in the biodegradation of aromatic molecules as compared to extradiol cleavage, extensive investigation of intradiol dioxygenases has been made due to the rich spectral properties of the iron(III) active site in the enzymes.[14–16]

Many $[FeN_6]^{2+}$ systems are based on the cationic low-spin $[Fe(2,2'\text{-bipyridine})_3]^{2+}$ or $[Fe(2,2':2',6'\text{-terpyridine})_2]^{2+}$ ions, where the critical field strength to reach the crossover condition is fulfilled by introducing sterically hindering groups adjacent to the donor atoms or by replacing the pyridine rings by five-membered heterocycles.[18] Examples are the spin crossover systems tris(6-methyl-2,2′-bipyridine)iron(II) and bis(2,4-bis(pyridin-2-yl)thiazole) iron(II) ions.[19] In view of the great importance of oxidation reactions in industrial and synthetic processes and of the ongoing search for new and efficient oxidation catalysts, we have synthesized and structurally characterized an iron(II)–phenanthroline complex. Electron paramagnetic resonance indicates the existence of a low-spin form of the iron complex at room temperature and points to its inactive behaviour towards 3,5-di-*tert*-butylcatechol (3,5-DTBC) under normal conditions. The complex acts as a functional model of catecholase enzyme using 3,5-DTBC as the model substrate through radical pathways with a significant turnover number (k_{cat} = 3.55 × 10^3 h^{-1}) and exhibits catechol dioxygenase activity towards the same 3,5-DTBC substrate at room temperature in oxygen-saturated ethanol medium.

Experimental

Materials

High purity 1,10-phenanthroline (phen; Aldrich, USA), ferric chloride (Merck, India), 3,5-DTBC (Sigma Aldrich Corporation, St Louis, MO,

* *Correspondence to: Bhaskar Biswas, Department of Chemistry, Raghunathpur College, Purulia 723133, India. E-mail:icbbiswas@gmail.com; mr.bbiswas@rediffmail.com*

a *Department of Chemistry, Raghunathpur College, Purulia 723133, India*

b *Department of Chemical Sciences, Indian Institute of Science Education and Research Mohali, Sector 81, S. A. S. Nagar, Manauli PO, Mohali 140306, India*

USA) and other materials were obtained from commercial sources and used as purchased. All other chemicals and solvents were of analytical grade and were used as received without further purification.

Preparation of $[Fe(phen)_3]Cl_2$ (1)

A methanolic solution (10 ml) of phen (0.540 g, 3 mmol) was added dropwise to a solution of $FeCl_3$ (0.163 g, 1 mmol) in the same solvent (10 ml) and the solution was refluxed for 30 min. The red coloured solution was kept in air for slow evaporation to obtain crystalline product.

Yield: 0.127 g (77.9% based on metal salt). Anal. Calcd for $C_{36}H_{24}N_6Cl_2Fe$ (**1**) (%): C, 64.79; H, 3.62; N, 12.59. Found (%): C, 64.71; H, 3.68; N, 12.64. IR (KBr, cm^{-1}): 1618, 1602 ($\nu_{C=N}$). UV–visible (λ_{max}, nm): 227, 266, 294, 323,512. EI-MS (*m/z*): 597.34 $[\mathbf{1} + H^+]^+$.

Physical measurements

Elemental analyses (carbon, hydrogen and nitrogen) were performed with a PerkinElmer 2400 CHNS/O elemental analyser. Fourier transform infrared (FT-IR) spectra (KBr discs, 300–4000 cm^{-1}) were recorded using a Shimadzu FTIR-8400S spectrophotometer. Ground-state absorption measurements were made with a JASCO model V-730 UV–visible spectrophotometer. ^1H NMR spectra were recorded with a Bruker DPX 500 MHz spectrometer. Electron paramagnetic resonance (EPR) spectra were recorded with a Bruker EMX-X band spectrometer. Electrospray ionization (EI) mass spectra were recorded using a Q-tof-micro quadruple mass spectrometer.

X-ray diffraction study

Single-crystal X-ray diffraction data of the iron(II) complex were collected using a Rigaku XtaLABmini diffractometer equipped with a Mercury CCD detector. The data were collected with graphite monochromated Mo Kα radiation (λ = 0.71073 Å) at 100 K using ω scans. The data were reduced using CrystalClear suite 2.0[20] and space group determination was done using Olex2. The structure was resolved by direct method and refined by full-matrix least-squares procedures using the SHELXL-2014/7[21] software package through the Olex^2 suite.[22] The crystallographic bond distances and bond angles were calculated using PARST.[23]

Catecholase activity of complex 1

In order to examine the catecholase activity of the complex, a 10^{-4} M solution of **1** in ethanol solvent was treated with 100 equiv. of 3,5-DTBC under aerobic conditions in the presence of triethylamine at room temperature. Absorbance versus wavelength (wavelength scans) of these solutions was recorded at a regular time interval of 5 min in the wavelength range 300–1000 nm. It may be noted here that a blank experiment without catalyst did not show formation of the quinone up to 6 h in ethanol. Kinetic experiments were performed spectrophotometrically with complex **1** and the substrate 3,5-DTBC in ethanol at 25 °C. An amount of 0.04 ml of the complex solution, with a constant concentration of 1×10^{-4} M, was added to 2 ml of 3,5-DTBC of a particular concentration (varying from 1×10^{-3} to 1×10^{-2} M) to achieve an ultimate concentration of the complex of 1×10^{-4} M. The conversion of 3,5-DTBC to 3,5-DTBQ (quinone band maxima) was monitored with time at a wavelength of 400 nm (time scan) in ethanol medium. The initial rate method was applied to determine the rate constant value for each concentration of the substrate and each experiment was repeated thrice.

Detection of presence of hydrogen peroxide in catalytic oxidation of 3,5-DTBC

To detect the formation of hydrogen peroxide during the catecholase reaction of **1**, we followed a reported method.[24] Reaction mixtures were prepared as in the kinetic experiments. During the course of the oxidation reaction, the solution was acidified with H_2SO_4 to pH 2 to stop further oxidation after a certain time and an equal volume of water was added. The formed quinone was extracted three times with dichloromethane. To the aqueous layer were added 1 ml of a 10% solution of KI and three drops of a 3% solution of ammonium molybdate. The formation of I_3^- could be monitored spectrophotometrically because of the development of the characteristic I_3^- band (λ_{max} = 353 nm).

Catechol dioxygenase activity of complex 1

To investigate the catechol dioxygenase activity of the complex, a 10^{-3} M solution of **1** in ethanol solvent was treated with a 10^{-3} M solution of DTBC in oxygen-saturated ethanol medium at room temperature. Absorbance versus wavelength (wavelength scans) of the solution was recorded at regular time intervals for 6 h in the wavelength range 200–900 nm. It may be noted here that a blank experiment without catalyst did not show the formation of any cleavage products up to 12 h in ethanol. The solvent was equilibrated at the atmospheric pressure of O_2 at 25 °C using a known procedure with modifications.[25,26] Investigation of dioxygen reactivity of the *in situ* generated Fe(III)–catecholate adduct was carried out in oxygen-saturated ethanol medium at 25 °C. Kinetic analyses[27,28] of the catechol cleavage reactions were carried out by time-dependent measurement of the disappearance of the lower energy DBC^{2-}-to-iron(III) ligand-to-metal charge transfer (LMCT) band at ambient temperature (25 °C) by exposure to molecular oxygen.

Determination of 3,5-DTBC cleavage products

An amount of 0.2548 g (0.04 mmol) of the iron(II) complex **1** was reacted with 0.088 g (0.04 mmol) of 3,5-DTBC in oxygen-saturated ethanol (100 ml) at ambient condition and then allowed to stir for 12 h. The red solution slowly turned green. The residue was then treated with 15 ml of 3 M HCl and the catechol cleavage products were extracted with diethyl ether (3 × 10 ml) and dried over sodium sulfate. The catechol cleavage products were analysed using electrospray ionization (ESI)-MS and were quantified using ^1H NMR spectroscopy. ^1H NMR data for 3,5-DTBC cleavage products (500 MHz, $CDCl_3$, δ, ppm): 3,5-di-*tert*-butyl-5-(carboxymethyl)-2-furanone: 6.89 (s, 1H); 3,5-di-*tert*-butyl-2-pyrone: 6.05 (m, 2H); 4,6-di-*tert*-butyl-2-pyrone: 7.23 (d,1H), 7.25 (d, 1H); 3,5-di-*tert*-butylbenzoquinone: 6.18 (d, 1H), 6.76 (d, 1H).

Results and discussion

Synthesis of Fe(II) complex 1 and spectroscopic characterization

The mononuclear iron(II)–phenanthroline complex was synthesized and isolated in crystalline phase from $FeCl_3$ with mixing of phen in an aqueous methanol medium under refluxing condition. The

geometry of the metal complex (**1**) was determined using single-crystal X-ray diffraction along with routine spectroscopic and analytical techniques.

The FT-IR spectrum of **1** (Fig. S1) contains characteristic strong bands for the 1,10-phen ligands, which shows characteristic bands for the α-diimine ligands at *ca* 1600 cm^{-1}.[29] In the higher-energy region of the optical spectrum, **1** shows characteristic bands at 266, 294 and 323 nm which are assignable to π–π* transition of the C=N chromophore in phen while a low-intensity broad band centred at 512 nm is observed in the visible region (Fig. S2), suggesting octahedral geometry around the iron centre.[30] The structural integrity in solution state for the iron(II) complex was determined using ESI-MS analysis. The mass spectrum of **1** in ethanol medium exhibits a molecular ion peak at *m/z* 597.34 as $[[Fe(phen)_3]^{2+} - H^+]^+$ (Fig. S3). The stability of the primary zone of coordination in the form of tris(phenanthroline)iron complex is also evident from the ESI-MS spectrum.

EPR spectroscopy experiments on **1** in ethanol medium at room temperature remain silent (Fig. S4) and indicate the low-spin conformation of complex **1**. The ^{1}H NMR spectrum of the iron complex in DMSO-d_6 testifies to its diamagnetic nature. The ^{1}H NMR spectrum of the complex (Fig. S5) contains characteristics peaks for aromatic protons in the region from *ca* 7 to 6 ppm for the phen ligands which further confirms its solution stability.

Description of crystal structure

The molecular structure of iron(II) complex **1** was determined using the single-crystal X-ray diffraction technique. Crystallographic data and details of data collection and refinement for **1** are presented in Table 1. Important bond lengths and angles are summarized in Table 2. Single-crystal analysis of complex **1** reveals that the compound crystallizes in the monoclinic system with C2/m space group. The ORTEP diagram of the complex cation of **1** is shown in Fig. 1. Each Fe(II) ion is coordinated by six N atoms of three phen ligands to form a distorted octahedral environment. The Fe1–N3 bond length, 1.988(6) Å, is slightly longer than that of the other Fe–N bonds; the average Fe–N bond length is 1.973 Å, in agreement with previously reported results for analogous compounds.[31] The mean value of the N–Fe–N bite angle in the bidentate ligands is 82.77° and the average *trans* angle for opposite N atoms in the coordination polyhedra is 175.85°, which is consistent with those found in similar complexes.[31] The bond lengths of all C=C & C=N in phen fall within the range of literature values.[32]

Table 1. Crystallographic refinement parameters of $[Fe(phen)_3]Cl_2$ (**1**)

Crystal parameter	**1**
Empirical formula	$C_{36}H_{24}N_6Cl_2Fe$
Formula weight	637.41
Temperature	100.0(2) K
Wavelength	0.71073 Å
Crystal system	Monoclinic
Space group	C2/m
Unit cell dimensions	a = 23.694(11) Å; α = 90.0°
	b = 20.786(16) Å; β = 106.533(16)°
	c = 15.304(6) Å; γ = 90.0°
Volume	7226(5) $Å^3$
Z	8
Density (calculated)	1.162 Mg m^{-3}
Absorption coefficient	0.522 mm^{-1}
F(000)	2600
Reflections collected	34 847
Independent reflections	8496
R(int)	0.066
Completeness to θ	99.4%
Goodness-of-fit on F^2	1.085
R indices (all data)	R_1 = 0.0813, wR_2 = 0.2637
Largest diff. Peak and hole	1.68 and −0.56 e $Å^{-3}$

Table 2. Selected bond distances (Å) and angles (°) for **1**

Bond distances			
N1–Fe1	1.968(4)	N4–Fe1	1.981(3)
N2–Fe1	1.967(4)	N5–Fe1	1.968(3)
N3–Fe1	1.988(4)	N6–Fe1	1.971(3)
Bond angles			
N1–Fe1–N2	82.92(14)	N2–Fe1–N3	91.73(13)
N1–Fe1–N3	91.71(13)	N2–Fe1–N4	91.98(13)
N1–Fe1–N4	172.28(13)	N2–Fe1–N5	94.55(13)
N1–Fe1–N5	94.48(13)	N2–Fe1–N6	175.85(13)
N1–Fe1–N6	94.25(14)	N4–Fe1–N5	91.70(13)
N3–Fe1–N4	82.62(13)	N4–Fe1–N6	91.14(14)
N3–Fe1–N5	171.67(14)	N5–Fe1–N6	82.62(13)
N3–Fe1–N6	91.38(13)		

Enzyme kinetics study including spectrophotometric investigation

In order to investigate the efficiency of catecholase activity of complex **1**, 3,5-DTBC with two bulky *t*-butyl substituents on the ring and low quinone–catechol reduction potential has been chosen as substrate. These properties of the substrate help it to undergo easy oxidation (Scheme 1) to the corresponding *o*-quinone, 3,5-DTBQ, which is highly stable and shows a maximum absorption in the wavelength range 380–420 nm.[24,33–35]

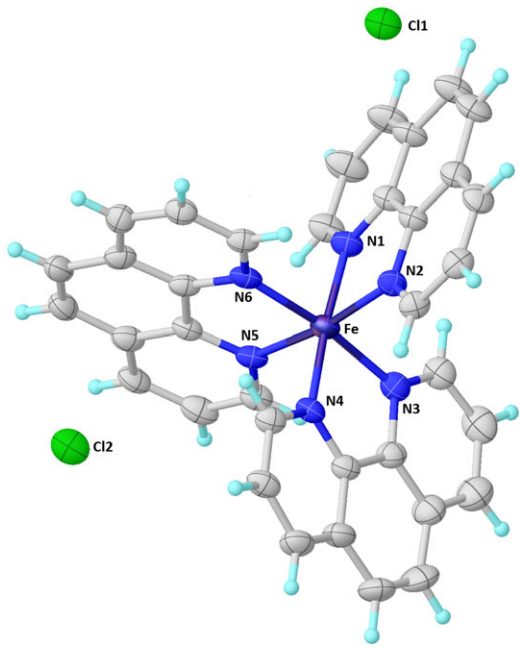

Figure 1. ORTEP diagram of the crystal structure of **1**.

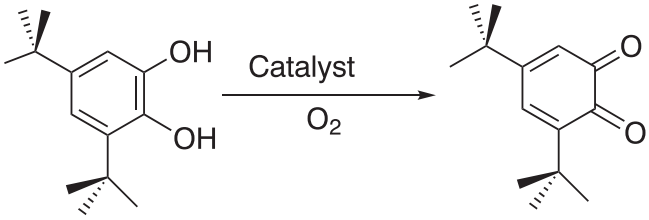

Scheme 1. Catalytic oxidation of 3,5-DTBC to 3,5-DTBQ in ethanol medium.

The catecholase activity of iron(II) complex **1** was studied using 3,5-DTBC as a convenient model substrate, in air-saturated ethanol solvent at room temperature. For this purpose, a 1×10^{-4} M solution of this complex was treated with 1×10^{-2} M (100 equiv.) 3,5-DTBC and the course of the reaction was followed by recording the UV–visible spectra of the mixture at intervals of 5 min for 2 h. At 25 °C under aerobic conditions, complex **1** shows inactive behaviour towards the model substrate, but instantly exhibits catechol oxidation activity in the presence of triethylamine. Spectral bands at 227, 266, 294, 323 and 512 nm appear in the electronic spectrum of complex **1** in ethanol, whereas 3,5-DTBC shows a single band at 284 nm. After the addition of triethylamine, there is a gradual decrease in intensity of the band at 284 nm due to the catechol[36] and a new band maximum is formed at 400 nm (Fig. 2) along with the generation of an isobestic point at *ca* 610 nm (Fig. 3). The experiment unequivocally proves catalytic oxidation of 3,5-DTBC to 3,5-DTBQ by the mononuclear Fe(II)–phen complex. The formed quinone derivative 3,5-DTBQ was purified by column chromatography using hexane–ethyl acetate eluent mixture. The product was isolated by slow evaporation of the eluent and was identified using H^1 NMR spectroscopy. ^{1}H NMR ($CDCl_3$, 400 MHz, δ_H, ppm): 1.16 (s, 9H), 1.20 (s, 9H), 6.15 (d, J = 2.4 Hz, 1H), 6.86 (d, J = 2.4 Hz, 1H).

The kinetics of the oxidation of 3,5-DTBC were determined by the method of initial rates and involved monitoring the growth of the quinone band at 400 nm as a function of time.[37] The complex shows saturation kinetics where a mechanism based on the Michaelis–Menten model seemed to be appropriate. The values of the Michaelis binding constant (K_m), maximum velocity (V_{max}) and rate constant for dissociation of substrate (i.e. turnover number, k_{cat}) were calculated for the complex **1** from graphs of $1/V$ versus $1/[S]$ (Fig. S6), known as Lineweaver–Burk graphs, using the equation $1/V = \{K_m/V_{max}\}\{1/[S]\} + 1/V_{max}$. The turnover number ($k_{cat}$) for the Fe(II) complex is 3.55×10^3 h^{-1} in ethanol. The kinetic parameters of **1** are also presented in Table 3.

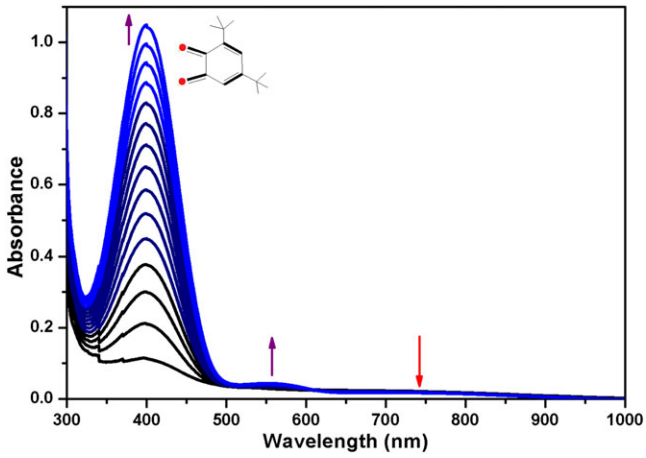

Figure 2. Increase of quinone band at 400 nm after addition of 100 equiv. of 3,5-DTBC to a solution containing **1** (10^{-4} M) in ethanol at 25 °C. The spectra were recorded every 5 min.

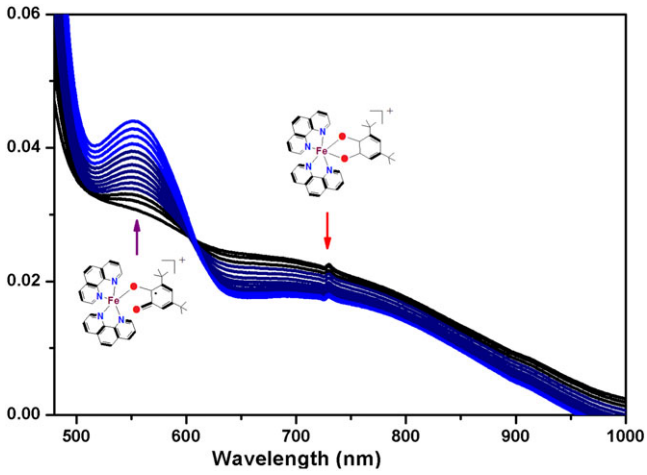

Figure 3. Increase of Fe(II)–semiquinone band with decrease of Fe(III)–catecholate band in the expansion of the wavelength range showing the presence of an isobestic point during the investigation of catecholase activity.

Mechanistic pathway for catecholase activity

Complex **1** in ethanol medium is a d^6 low-spin system and exhibits chemical inertness in ethanolic solution. But, upon addition of 3,5-DTBC to **1** in the presence of an organic base, triethylamine, the effective *in situ* generation of the Fe(III)–catecholate adduct is observed which is also evident from EPR spectral analysis of the reaction mixture at room temperature. Though the EPR spectrum of the iron(II) complex in ethanol medium remains silent (Fig. S4) under normal conditions, upon addition of 3,5-DTBC to **1** in the presence of triethylamine, it displays high-spin (S = 5/2) rhombic ferric signals[38,39] at g = 7.9, 4.3, 2.1 (Fig. S4). Triethylamine, being an organic base, helps to abstract the protons from phenolic-OH groups and enhances the nucleophilicity on oxygen atoms. As a result, the substrate now acts as a better chelating ligand and facilitates the formation of iron(III)–catecholate adduct. To establish the pathway for the catalytic reaction, we initially detected the presence of hydrogen peroxide following a reported procedure[24] and observed the band at 353 nm which is due to I_3^- (see Experimental section; Fig. S7). To obtain a mechanistic inference of the catecholase activity of **1** and to confirm possible complex–substrate intermediates, we recorded the ESI-MS spectrum for a 1:100 mixture of the complex and 3,5-DTBC within 10 min of mixing in an ethanol solvent. ESI-MS analysis (Fig. S8) of the reaction

Table 3. Kinetic parameters for the oxidation of 3,5-DTBC catalysed by **1** in ethanol

Molecular formula	V_{max} (M s^{-1})	K_m (M)	k_{cat} (h^{-1})	Ref.
$C_{36}H_{24}N_6Cl_2Fe$[a]	9.87×10^{-5}	1.06×10^{-2}	3.55×10^3	This work
$C_{42}H_{44}N_6O_{10}Fe_2$	2.08×10^{-5}	4.38×10^{-4}	7.51×10^2	[40]
$C_{75}H_{42}O_{71}Fe_{11}$	8.91×10^{-5}	3.15×10^{-3}	3.21×10^3	[41]
$C_{35}H_{49}Cl_3N_4O_{11}Fe_2$	—	7.30×10^{-3}	3.43×10^4	[42
$C_{35}H_{36}N_4O_3Fe_2$	—	7.10×10^{-2}	4.16×10^4	[43]

[a]Standard error for V_{max} (M s^{-1}) = 1.24×10^{-5}; standard error for K_m (M) = 3.21×10^{-3}.

Applied Organometallic Chemistry

mixture reveals that enzyme–substrate binding occurs in solution and the presence of an isobestic point at *ca* 610 nm is further evident. The mass spectrum of the reaction mixture supports the existence of mononuclear Fe(III)–catecholate adduct, {[Fe(phen)$_2$(DTBC)]H$^+$} at *m/z* 637.34, {[Fe(O$_2$)(phen)$_2$(DTBC)]H$^+$} at *m/z* 670.25 and [Na(DTBQ)]$^+$ at *m/z* 243.10 in ethanol solution. During the course of catechol oxidation, an intense catecholate-to-iron(III) LMCT band at *ca* 718 nm[39] with gradual decrease in intensity (Fig. 3) and a Fe(II)–semiquinone band[38] with gradual increase in intensity at *ca* 548 nm (Fig. 3) are also observed for **1**. This spectrophotometric investigation indicates that the Fe(III)–catecholate species and Fe(II)–semiquinone species form a valence tautomerism, and the reactive intermediate species exist in an equilibrium which is also confirmed by the presence of an isobestic point at *ca* 610 nm. Benzoquinone as major product is a result of this course of catalysis. Moreover, in the catalytic reaction, when performed in an inert atmosphere, no 3,5-DTBQ formation is observed. However, upon exposure of the reaction mixture to dioxygen atmosphere, immediately 3,5-DTBQ formation is noticed. This observation indeed indicates that dioxygen is one of the active participants in the catalytic cycle and it converts the semibenzoquinone radical to the quinone with hydrogen peroxide. The catalytic cycle favouring the catecholase activity is shown in Scheme 2.

To investigate the efficiency of the catalytic activity we draw a comparison between our complex **1** and some recently reported iron complexes which show efficient catecholase activity (Table 3).[40–43] This comparison also indicates that complex **1** acts as a better and effective catalyst towards catecholase activity than the reported ones.[40–43]

Catechol dioxygenase activity of complex 1

The oxygenation reactions with the iron(II) complex were carried out using 3,5-DTBC as the model substrate in bio-friendly ethanol. The advantages of using the latter as substrate are the relatively high stability of the main cleavage product and the fast reaction of the catecholate complex with dioxygen at room temperature. The DTBC^{2-} adducts of the iron(II) complex were generated *in situ* in ethanol solution, and their reactivity towards O$_2$ was investigated

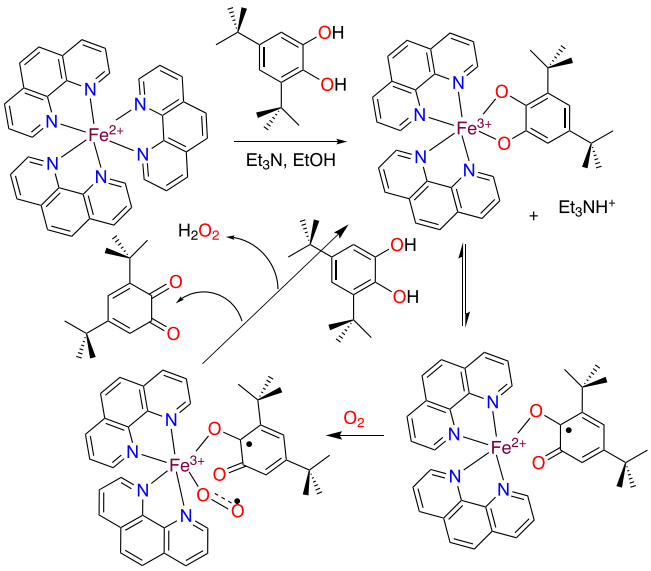

Scheme 2. Mechanistic aspects in favour of catecholase activity by iron complex.

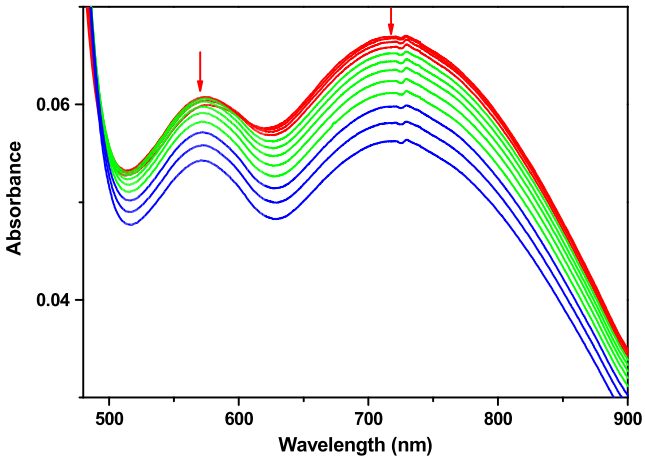

Figure 4. Absorption spectral changes during the reaction of the *in situ* generated adduct [Fe(phen)$_2$(DBC)]$^+$ with O$_2$ (the spectra were recorded every 12 min).

by monitoring the decay of the low-energy DTBC^{2-}-to-Fe(III) LMCT band (Fig. 4). The presence of an isobestic point during the investigation of catecholase activity further supports the effective formation of iron–catecholate intermediate which also remains one of the fundamental aspects for the conversion of substrate to product and catalytic efficacy of the metal complex. The red solution of **1** reacts with dioxygen in bio-friendly ethanol medium at ambient conditions over a period of 6 h and two new visible bands with maximum absorption at 575 and 721 nm (Fig. 4) are observed for the catecholate adduct of complex **1**. The lower energy visible bands decreasing in absorbance are attributed to 3,5-DTBC^{2-}-to-iron(III) LMCT transitions involving two different catecholate ligand orbitals.[5–8,28,38,39,44] As reported in many cases, the energy of the LMCT transitions strongly depends on the nature of the ligands, and it reflects the Lewis acidity of the iron centre in the complex.[5,6,45] The disappearance of the lower energy catecholate-to-iron(III) LMCT band (Fig. 4) on oxygenation exhibits pseudo first-order kinetics, as judged from the linearity of a plot of [1 + log(absorbance)] versus time[39,44] (Fig. 5), and the value of k_{obs} is obtained from the slope of the plot. The pseudo first-order rate constant is determined as $k_{obs} = 9.89 \times 10^{-4}$ min^{-1}.

Further, the oxidized products (Scheme 3) from catechol-bound Fe(III) species were identified and quantified using ^{1}H NMR

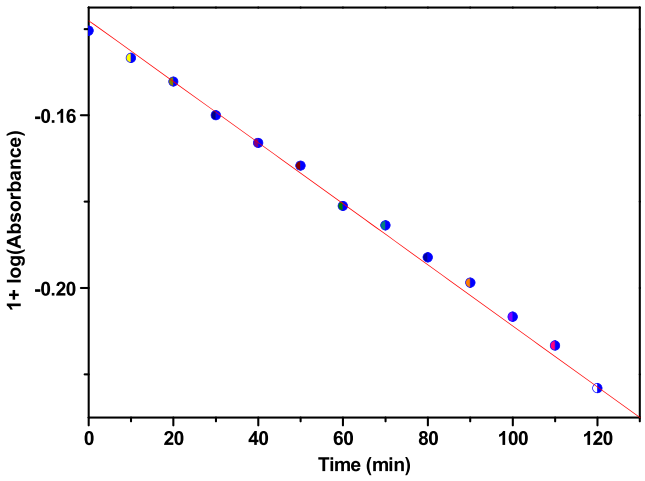

Figure 5. Plot of [1 + log(absorbance)] versus time for the reaction of [Fe(phen)$_2$(DTBC)]$^+$ with O$_2$ at 25 °C in ethanol solution.

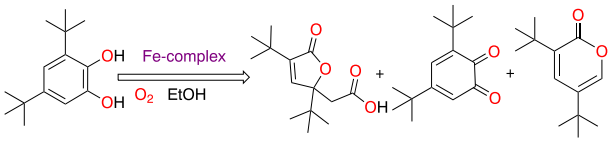

Scheme 3. Oxygenation products of DTBC for iron complex in ethanol.

spectroscopy (Fig. S9) and ESI-MS (Fig. S10). The distribution of catechol-derived products is found to be mainly 3,5-di-*tert*-butyl-5-(carboxymethyl)-2-furanone as intradiol cleavage product in major amount and 3,5-di-*tert*-butylbenzoquinone as minor product, while 4,6-di-*tert*-butyl-2-pyrone and 3,5-di-*tert*-butyl-2-pyrone, as extradiol cleavage products, are found in trace quantities. In the reaction of (**1** + DTBC) with O_2 in bio-friendly ethanol, 73% of intradiol cleavage product is obtained along with the formation of small amounts of extradiol cleavage products (5.3% + 2.4%) as side products. The amount of minor oxidation product, 3,5-di-*tert*-butylbenzoquinone, is also found to be small (11.4%). The amount of organic product from catechol cleavage accounts for *ca* 93% of 3,5-DTBC. The remaining 7% is accounted for unreacted substrate.

The formation of intradiol cleavage products for the catecholate adduct of the iron(II) complex is expected of the six-coordinate geometry, which favours a substrate-activation[46,47] rather than dioxygen-activation[48–50] pathway as the latter requires a vacant coordination site on the catecholate adduct for oxygen coordination followed by activation. The observation of smaller amounts of extradiol products for this iron(II) complex may be explained by invoking the partial displacement of the phen ligand from the coordination sphere containing more Lewis basic ligand donors (ethanol), which facilitates dioxygen attack on iron(III) for extradiol cleavage to occur.

From ESI-MS analysis of the reaction mixture it is revealed that, at the primary stage, 3,5-DTBC behaves as a bidentate chelator towards mononuclear Fe(II) complex and turns into an octahedral Fe(III)–catecholate adduct, which exhibits no preference for molecular oxygen activation. But the existence of iron(II)–semiquinone species in solution facilitates a substrate activation mechanism and provides one electron from Fe(II) to the anti-bonding orbital of dioxygen generating oxo-species in solution. Further, the acyl group migration produces the intradiol cleavage products and hydrogen peroxide. Probably, the intradiol catechol cleavage reaction proceeds by an iron(III) peroxo intermediate that undergoes 1,2-Criegee rearrangement to yield the intradiol catechol cleaved products analogous to the native enzyme.

Conclusions

A mononuclear iron(II)–phrenanthroline complex was synthesized and characterized using various spectroscopic methods. Single-crystal X-ray diffraction analysis revealed that **1** crystallizes in a monoclinic system with C2/m space group. The iron(II) complex is stable in ethanolic medium, but upon addition of 3,5-DTBC pretreated with two equivalents of triethylamine, the diamagnetic iron(II) compound converts into a mononuclear paramagnetic Fe(III)–catecholate species. The complex acts as a functional model for a biomimetic catalyst promoting the aerobic oxidation of 3,5-DTBC through radical pathways with a significant turnover number ($k_{cat} = 3.55 \times 10^3\ h^{-1}$) and exhibits catechol dioxygenase activity towards the same substrate, i.e. 3,5-DTBC, at room temperature in oxygen-saturated ethanol medium. The existence of an isobestic point at 610 nm from spectrophotometric data supports the presence of Fe^{3+}–3,5-DTBC adduct favouring enzyme–substrate binding and the occurrence of a valence tautomerism between Fe(II)–semiquinone and Fe(III)–catecholate species. Upon stoichiometric addition of 3,5-DTBC pretreated with two equivalents of triethylamine to the iron complex, two catecholate-to-iron(III) LMCT bands (575 and 721 nm) are observed and the *in situ* generated catecholate intermediate reacts with dioxygen ($k_{obs} = 9.89 \times 10^{-4}\ min^{-1}$) in ethanol medium to afford exclusively intradiol cleavage products along with a small amount of benzoquinone and a small amount of extradiol cleavage products which provide substantial evidence for the substrate activation mechanism. Complex **1** is a new addition to the class of oxidase and dioxygenase enzymes with good catalytic activity and functional biomimicking efficacy.

Acknowledgements

The work was supported financially by the Science & Engineering Research Board (SERB), New Delhi, India under Fast Track Scheme for Young Scientist (no. SB/FT/CS-088/2013 dtd.21/05/2014). BB is grateful to IACS, Kolkata for providing EPR analysis, ^{1}H NMR and mass spectrometry. HRY thanks UGC for a fellowship and ARC thanks IISER Mohali for the use of the departmental X-ray facility.

References

[1] R. H. Prince, in *Comprehensive Coordination Chemistry*, Vol. *5* (Eds: G. Wilkinson, R. Gillard, J. A. McCleverty), Pergamon, Oxford, **1987**, p. 925.
[2] B. Biswas, M. Mitra, J. Adhikary, G. R. Krishna, P. P. Bag, C. M. Reddy, N. Aliaga-Alcalde, T. Chattopadhyay, D. Das, R. Ghosh, *Polyhedron* **2013**, *53*, 264.
[3] B. Biswas, A. Al-Hunaiti, M. T. Räisänen, S. Ansalone, M. Leskelä, T. Repo, Y.-T. Chen, H.-L. Tsai, A. D. Naik, A. P. Railliet, Y. Garcia, R. Ghosh, N. Kole, *Eur. J. Inorg. Chem* **2012**, 4479.
[4] A. L. Feig, S. J. Lippard, *Chem. Rev.* **1994**, *94*, 759.
[5] E. L. Hegg, L. Que, Jr., *Eur. J. Biochem.* **1997**, *250*, 625.
[6] J. D. Lipscomb, A. M. Orville, in *Metal Ions in Biological Systems*, Vol. *28* (Eds: H. Sigel, A. Sigel), Marcel Dekker, New York, **1992**, p. 243.
[7] L. Que, Jr., R. Y. N. Ho, *Chem. Rev.* **1996**, *96*, 2607.
[8] L. Que, Jr., J. D. Lipscomb, E. Münck, J. M. Wood, *Biochim. Biophys. Acta* **1977**, *485*, 60.
[9] L. Que, Jr., in *Iron Carriers and Iron Proteins* (Ed: T. M. Loehr), VCH, New York, **1989**, p. 467.
[10] D. H. Ohlendorf, J. D. Lipscomb, P. C. Weber, *Nature* **1988**, *336*, 403.
[11] D. H. Ohlendorf, A. M. Orville, J. D. Lipscomb, *J. Mol. Biol.* **1994**, *244*, 586.
[12] M. P. Valley, C. K. Brown, D. L. Burk, M. W. Vetting, D. H. Ohlendorf, J. D. Lipscomb, *Biochemistry* **2005**, *44*, 11024.
[13] R. W. Frazee, A. M. Orville, K. B. Dolbeare, H. Yu, D. H. Ohlendorf, J. D. Lipscomb, *Biochemistry* **1998**, *37*, 2131.
[14] M. W. Vetting, D. A. D'Argenio, L. N. Ornston, D. H. Ohlendorf, *Biochemistry* **2000**, *39*, 7943.
[15] M. W. Vetting, D. H. Ohlendorf, *Structure* **2000**, *8*, 429.
[16] J. W. Whittaker, J. D. Lipscomb, *J. Biol. Chem.* **1984**, *259*, 4487.
[17] A. M. Orville, J. D. Lipscomb, D. H. Ohlendorf, *Biochemistry* **1997**, *36*, 10052.
[18] P. Gütlich, Y. Garcia, H. A. Goodwin, *Chem. Soc. Rev.* **2000**, *29*, 419.
[19] B. J. Childs, D. C. Craig, M. L. Scudder, H. A. Goodwin, *Inorg. Chim. Acta* **1998**, *274*, 32.
[20] CrystalClear 2.0, Rigaku Corporation, Tokyo, Japan.
[21] G. M. Sheldrick, *Acta Crystallogr. A* **2008**, *64*, 112.
[22] O. V. Dolomanov, L. J. Bourhis, R. J. Gildea, J. A. K. Howard, *H. Puschmann. J. Appl. Crystallogr* **2009**, *42*, 339.
[23] M. Nardelli, *Comput. Chem.* **1983**, *7*, 95.
[24] D. Dey, S. Das, H. R. Yadav, A. Ranjani, L. Gyathri, S. Roy, P. S. Guin, D. Dhanasekaran, A. R. Choudhury, M. A. Akbarsha, B. Biswas, *Polyhedron* **2016**, *106*, 106.
[25] D. T. Sawyer, *Oxygen Chemistry*, Oxford University Press, New York, **1991**.

[26] P. Mialane, L. Tehertanov, F. Banse, J. Sainton, J. Girerd, *Inorg. Chem.* **2000**, *39*, 2440.
[27] P. Halder, S. Paria, T. K. Paine, *Chem. Eur. J* **2012**, *18*, 11778.
[28] R. Mayilmurugan, K. Visvaganesan, E. Suresh, M. Palaniandavar, *Inorg. Chem.* **2009**, *48*, 8771.
[29] K. Nakamoto, *Infrared and Raman Spectra of Inorganic and Coordination Compounds: Part B, Applications in Coordination, Organometallic and Bioinorganic Chemistry*, John Wiley, New York, **1997**, p. 116.
[30] J. G. Solé, L. E. Bausá, D. Jaque, *An Introduction to the Optical Spectroscopy of Inorganic Solids*, John Wiley, Chichester, **2005**.
[31] Q. X. Wang, K. Jiao, W. Sun, F. F. Jian, X. Hu, *Eur. J. Inorg. Chem* **1838**, *2006*.
[32] Y. P. Tian, C. Y. Duan, X. X. Xu, X. Z. You, *Acta Crystallogr. C* **1995**, *51*, 2309.
[33] D. Dey, A. De, H. R. Yadav, P. S. Guin, A. R. Choudhury, N. Kole, B. Biswas, *ChemistrySelect* **2016**, *01*, 1910.
[34] S. Pal, B. Chowdhury, M. Patra, M. Maji, B. Biswas, *Spectrochim. Acta A* **2015**, *144*, 148.
[35] D. Dey, A. De, S. Pal, P. Mitra, A. Ranjani, L. Gayathri, S. Chandraleka, D. Dhanasekaran, M. A. Akbarsha, N. Kole, B. Biswas, *Indian J. Chem. A* **2015**, *54*, 170.
[36] D. Dey, G. Kaur, A. Ranjani, L. Gyathri, P. Chakraborty, J. Adhikary, J. Pasan, D. Dhanasekaran, A. R. Choudhury, M. A. Akbarsha, N. Kole, B. Biswas, *Eur. J. Inorg. Chem* **2014**, 3350.
[37] D. D. Cox, S. J. Benkovic, L. M. Bloom, F. C. Bradley, M. J. Nelson, L. Que, Jr., D. E. Wallick, *J. Am. Chem. Soc.* **1988**, *110*, 2026.
[38] T. Kurahashi, K. Oda, M. Sugimoto, T. Ogura, H. Fujii, *Inorg. Chem.* **2006**, *45*, 7709.
[39] R. Mayilmurugan, M. Sankaralingam, E. Suresh, *Palaniandavar, Dalton Trans* **2010**, *39*, 9610.
[40] M. Mitra, A. K. Maji, B. K. Ghosh, P. Raghavaiah, J. Ribas, R. Ghosh, *Polyhedron* **2014**, *67*, 19.
[41] S. K. Mal, M. Mitra, B. Biswas, G. Kaur, P. P. Bag, C. M. Reddy, A. R. Choudhury, N. A. Alcalde, R. Ghosh, *Inorg. Chim. Acta* **2015**, *425*, 61.
[42] T. P. Camargo, F. F. Maia, C. Chaves, B. de Souza, A. J. Bortoluzzi, N. Castilho, T. Bortolotto, H. Terenzi, E. E. Castellano, W. Haase, Z. Tomkowicz, R. A. Peralta, A. Neves, *J. Inorg. Biochem.* **2015**, *146*, 77.
[43] R. J. Souza, *Síntese, Caracterização e Avaliação da Promiscuidade Catalítica de Complexos Binucleares Bioinspirados*, Chemistry Department, Universidade Federal de Santa Catarina, Florianópolis, **2010**.
[44] M. Merkel, F. K. Müller, B. Krebs, *Inorg. Chim. Acta* **2002**, *337*, 308.
[45] J.-Y. Xu, J. Astner, O. Walter, F. W. Heinemann, S. Schindler, M. Merkel, B. Krebs, *Eur. J. Inorg. Chem* **1601**, *2006*.
[46] M. Pascaly, M. Duda, F. Schweppe, F. Zurlinden, K. Muller, B. Krebs, *J. Chem. Soc. Dalton Trans.* **2001**, 828.
[47] W. O. Koch, H.-J. Kruger, *Angew. Chem. Int. Ed. Engl.* **1995**, *34*, 2671.
[48] M. Ito, L. Que, Jr., *Angew. Chem. Int. Ed. Engl.* **1997**, *36*, 1342.
[49] T. Funabiki, A. Mizoguchi, T. Sugimoto, S. Tada, M. Tsuji, H. Sakamoto, S. Yoshida, *J. Am. Chem. Soc.* **1986**, *108*, 2921.
[50] A. Die, D. Gatteschi, L. Pardi, *Inorg. Chem.* **1993**, *32*, 1389.

Supporting information

Additional supporting information may be found in the online version of this article at the publisher's web-site.